



# Poly(3-hydroxybutyrate) nanocomposites: Isothermal degradation and kinetic analysis

Matko Erceg\*, Tonka Kovačić, Ivka Klarić

Department of Organic Technology, Faculty of Chemistry and Technology, University of Split, Teslina 10/V, 21 000 Split, Croatia

## ARTICLE INFO

### Article history:

Received 18 September 2008

Received in revised form

24 November 2008

Accepted 2 December 2008

Available online 11 December 2008

### Keywords:

Isothermal thermogravimetry

Kinetic analysis

Nanocomposites

Organically modified montmorillonite

Poly(3-hydroxybutyrate)

## ABSTRACT

Polymer nanocomposites consisted of biodegradable poly(3-hydroxybutyrate) (PHB) and organically modified montmorillonite Cloisite30B (30B) have been prepared by the solution casting method and isothermally degraded at 230, 235, 240 and 245 °C. The addition of 30B increases the thermal stability of PHB and the most pronounced effect has the addition of 1 wt.% of 30B. Kinetic analysis was performed using *model-free* isoconversional and reduced time plots (RTP) methods. The isothermal degradation of pure PHB and PHB/30B nanocomposites can be separated in two distinct regions: the first where small mass loss appears and the second, assigned as the main degradation mechanism, where the main mass loss takes place. The empirical kinetic triplets ( $E$ ,  $A$ , and  $g(\alpha)$ ) for the main degradation mechanism were determined.

© 2008 Elsevier B.V. All rights reserved.

## 1. Introduction

Poly(3-hydroxybutyrate) (PHB) is a fully biodegradable, thermoplastic aliphatic polyester with biocompatibility and ecological safety, produced in nature by at least 75 different genera of bacteria as an energy storage material [1]. Its physical properties are often compared to isotactic polypropylene since they have similar melting points and crystallinity [2]. However, it has several drawbacks, such as stiffness, brittleness and very low thermal stability at processing temperatures that prevent its larger commercial applications. The thermal instability of PHB in the melt prevents it from substituting the non-biodegradable polymeric materials in commercial products [3]. That is why improvement of the thermal stability of PHB is very important.

To overcome these drawbacks of PHB we have prepared PHB nanocomposites with organically modified montmorillonite [4]. Polymer nanocomposites are commonly defined as the combination of a polymeric matrix and fillers that have at least one dimension (i.e. length, width or thickness) in the nanometre size range [5]. It has been shown that only a few percent of nanofillers (usually from 1 to 5 wt.%) leads to greatly improved thermal, mechanical and barrier properties of polymers [6–8]. Commercially the most important type of polymer nanocomposites are those produced using layered clay minerals (2:1 phyllosili-

cates), especially montmorillonite. Montmorillonite is naturally abundant, environmentally friendly and economic. It is usually chemically modified by a cation-exchange method, by which its sodium counterions are exchanged with adequate organic, usually alkyl ammonium cations, in order to match its compatibility with polymer matrix what is the key to successful preparation of polymer nanocomposites [9]. In this work, PHB nanocomposites with organically modified montmorillonite Cloisite30B (30B) have been prepared. Then, we have isothermally degraded PHB/30B nanocomposites, investigated the influence of 30B on the thermal stability of PHB and performed the kinetic analysis of this process.

The aim of the kinetic analysis is determination of kinetic triplets (i.e. kinetic model,  $g(\alpha)$ , activation energy,  $E$ , and pre-exponential factor,  $A$ ) for the investigated process. It is suggested that prior to any kinetic analysis one should investigate the complexity of the process by determining the dependence of  $E$  on conversion,  $\alpha$  by isoconversional methods [10]. Namely, the dependence of  $E$  on  $\alpha$  is considered as reliable criterion of the process complexity [10] and isoconversional methods are considered as the most reliable methods for the calculation of  $E$  and  $E$  vs.  $\alpha$  dependence of thermally activated reactions [10,11]. If  $E$  does not depend on  $\alpha$ , the investigated process is simple (overall single-stage) and can be described by unique kinetic triplet. If  $E$  depends on  $\alpha$ , the process is complex and the shape of the curve  $E$  vs.  $\alpha$  indicates the possible reaction mechanism [10,11]. In this work,  $E$  values and  $E$  vs.  $\alpha$  dependence have been calculated by means of *model-free* isoconversional method.

\* Corresponding author. Tel.: +385 21 329 459; fax: +385 21 329 461.  
E-mail address: [merceg@ktf-split.hr](mailto:merceg@ktf-split.hr) (M. Erceg).

The reduced time plots (RTP) method has been used for the determination of kinetic model,  $g(\alpha)$  of the investigated process. RTP method is considered as one of the reliable tools for determination of kinetic models of the isothermal degradation and is broadly used in solid state kinetics [12,13]. Furthermore,  $E$  and  $A$  values corresponding to determined  $g(\alpha)$ , i.e. kinetic triplets, have been calculated.

## 2. Experimental

### 2.1. Materials and sample preparation

Poly(3-hydroxybutyrate) (PHB), kindly supplied by Biomer (Krailling, Germany), was used as received.  $\bar{M}_w$  of 350 000 was determined viscosimetrically (chloroform, 30 °C) using the equation  $[\eta] = 1.18 \times 10^{-4} \bar{M}_w^{0.78}$  [14]. Organically modified montmorillonite Cloisite30B (30B) was purchased from Southern Clay Products Inc. (Gonzales, USA) and used as received. It is a natural montmorillonite modified with dimethyl-2-ethylhexyl (hydrogenated tallowalkyl) ammonium cation and its properties can be found in [15].

PHB/30B nanocomposites (100/1, 100/3, 100/5, 100/7 and 100/10 by weight) were prepared by the solution-intercalation method. The detailed preparation procedure is described in our earlier work [4].

### 2.2. Thermal degradation

The PHB/30B samples (sample mass  $4.7 \pm 0.3$  mg) were isothermally degraded for 120 min at 230, 235, 240 and 245 °C in the nitrogen atmosphere ( $30 \text{ cm}^3 \text{ min}^{-1}$ ) using a Perkin-Elmer TGS-2 thermobalance. The samples were heated at a rate of  $80 \text{ °C min}^{-1}$  from the starting temperature (50 °C) to the temperature of the isothermal degradation. Before operating, the system was stabilised for 1 h.

## 3. Theory

Kinetic analysis of the solid state decompositions, like the isothermal degradation of PHB and its nanocomposites, is usually based on a single step kinetic equation:

$$\frac{d\alpha}{dt} = k(T)f(\alpha) \quad (1)$$

where  $t$  is time,  $T$  is temperature,  $k$  is rate constant,  $f(\alpha)$  is differential form of the kinetic model and  $\alpha$  is conversion defined as the ratio  $(m_0 - m)/(m_0 - m_f)$ , where  $m_0$ ,  $m$  and  $m_f$  refer to the initial, actual and residual mass of the sample.

Arrhenius equation expresses the explicit temperature dependence of the rate constant, which gives:

$$\frac{d\alpha}{dt} = A \exp\left(\frac{-E}{RT}\right) f(\alpha) \quad (2)$$

where  $A$  is the pre-exponential factor and  $R$  is the gas constant.  $E$ ,  $A$  and  $f(\alpha)$  are called kinetic triplet and can be used to kinetically describe the time evolution of a physical or chemical change of the solid-state reactions that are ruled by a overall single-stage process. Since the determination of  $E$ ,  $A$  and  $f(\alpha)$  of thermally activated reactions is interlinked problem, the kinetic analysis should start with determination of one element of the triplet with high accuracy [16] and that is  $E$ . As mentioned in Introduction, *model-free* isoconversional methods are considered as the most reliable methods for the calculation of  $E$  and  $E$  vs.  $\alpha$  dependence. For this purpose we have used *model-free* isoconversional method which is based on

the following equation:

$$\ln t = -\ln\left(\frac{A}{g(\alpha)}\right) + \left(\frac{E_{iso}}{R}\right) \frac{1}{T} \quad (3)$$

where  $g(\alpha)$  is the integral form of the kinetic model.

This method requires  $\alpha$  vs.  $t$  data from at least three different temperatures for determination of  $E_{iso}$ . For a constant value of  $\alpha$ , the first term in Eq. (3) is constant and  $E_{iso}$  can be determined from the slope of the straight line  $\ln t$  vs.  $1/T$ .

Reduced time plots (RTP) method has been applied to determine the reaction model of the investigated change. The experimental reduced time plots (RTPs) are developed by plotting  $\alpha$  as a function of a reduced time variable,  $t/t_\alpha$ , where  $t_\alpha$  is time required to obtain a specified conversion; in our case  $\alpha = 0.9$ . Here  $t_{0.9}$  has been chosen because final value of  $\alpha$  had crossed 0.9 in all cases. If the experimental RTPs are superimposable (i.e. with the limits of the reproducibility at individual temperatures) the kinetic model does not change with temperature of isothermal degradation. These experimental RTPs are compared with RTPs of the theoretical kinetic models. Each theoretical kinetic model has the unique RTP curve irrespective of the nature of the system, temperature and other factors which affect the reaction rate [17]. Therefore, the theoretical kinetic model that gives the best fit of the experimental results can be considered as true kinetic model of the investigated process. This is why this approach can be labelled as “model free” [18].

After determination of  $g(\alpha)$ , one can calculate the rate constants,  $k$  for each investigated temperature from the slope of the plot  $g(\alpha)$  vs.  $t$ :

$$g(\alpha) = k(T)t \quad (4)$$

These values of  $k$  are then used for calculation of  $E$  and  $A$  that corresponds to the determined kinetic model, from the slope and the intercept of Eq. (5), respectively:

$$\ln k(T) = \ln A - \frac{E}{R} \frac{1}{T} \quad (5)$$

In this way, the kinetic triplets of the investigated processes are calculated. In order to check their correctness,  $E$  values that correspond to the determined kinetic models are compared with  $E_{iso}$  values obtained by *model-free* isoconversional method. If the correct kinetic triplets have been determined,  $E$  and  $E_{iso}$  values should be similar.

## 4. Results and discussion

### 4.1. Isothermal thermogravimetry

Fig. 1 shows the isothermal TG curves of pure PHB at 200, 230, 235, 240 and 245 °C and PHB/30B 100/1 nanocomposites at 230, 235, 240 and 245 °C, while Fig. 2 shows the isothermal TG curves for all PHB/30B nanocomposites at 230 °C. Recommended temperature range for processing of PHB is 180–200 °C [19]. After 120 min of isothermal degradation at 200 °C the mass loss of pure PHB was 19 wt.% (Fig. 1). Since the addition of 30B has increased the thermal stability of PHB under the non-isothermal degradation [4], the same effect under isothermal conditions could be expected. Therefore, isothermal degradation of PHB and its nanocomposites should be performed at temperatures higher than 200 °C in order to investigate the whole degradation process in a reasonable time. Also, kinetic analysis is more useful if it is performed in the whole degradation range. We have chosen temperatures 230, 235, 240 and 245 °C for isothermal degradation of PHB/30B nanocomposites. At these temperatures the main reaction involves random chain scission as well as at the processing temperatures [19,20]. Also, at these temperatures the degradation rate of PHB is high enough and PHB

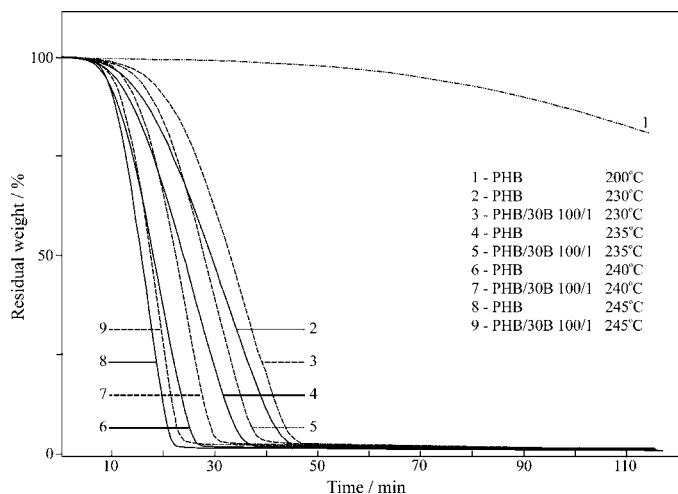


**Fig. 1.** The isothermal TG curves for pure PHB and PHB/30B 100/1 nanocomposites at 230, 235, 240 and 245 °C.

is completely volatilized, i.e. constant weight loss is established after 45, 36, 26 and 20 min at 230, 235, 240 and 245 °C, respectively (Fig. 1). Within 120 min at these temperatures constant weight loss is established for all other analysed samples what is necessary in order to use isothermal data for kinetic analysis.

It is obvious from Figs. 1 and 2 that addition of 30B in amounts up to 5 wt.% shifts the establishment of constant weight loss to longer degradation times compared to pure PHB, i.e. improves its thermal stability. The most pronounced effect has the addition of 1 wt.% of 30B when the establishment of constant weight loss is shifted up to 5 min towards longer degradation times compared to pure PHB. This shift depends on the temperature of isothermal degradation and is higher at lower degradation temperatures.

Increase in the thermal stability of polymer nanocomposites compared to pure polymer is usually attributed to the mass barrier effect of silicate layers to volatile products generated during thermal decomposition. Silicate layers are impermeable for volatile products [8,21] and labyrinth effect of the silicate layers may slow down their diffusion and delay the weight loss. Due to their high thermal stability, clay particles can also act as the thermal insulator but only if they are well dispersed in polymer matrix and in amounts below which their agglomeration occurs. The better the dispersion of nanofiller is achieved, the more significant enhancement of ther-

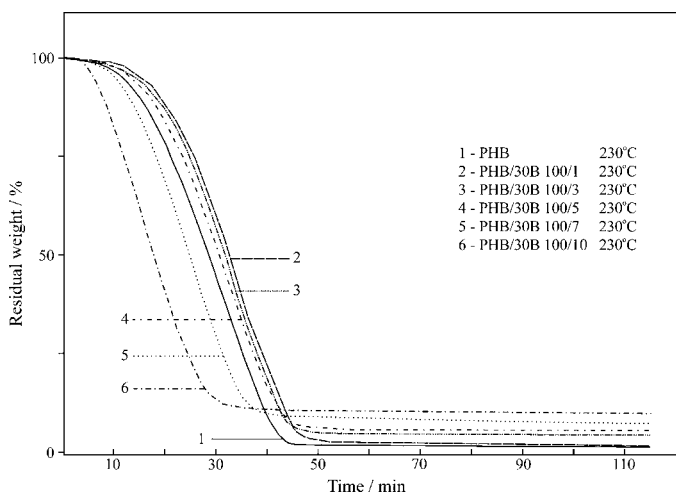


**Fig. 2.** The isothermal TG curves for pure PHB and PHB/30B nanocomposites at 230 °C.

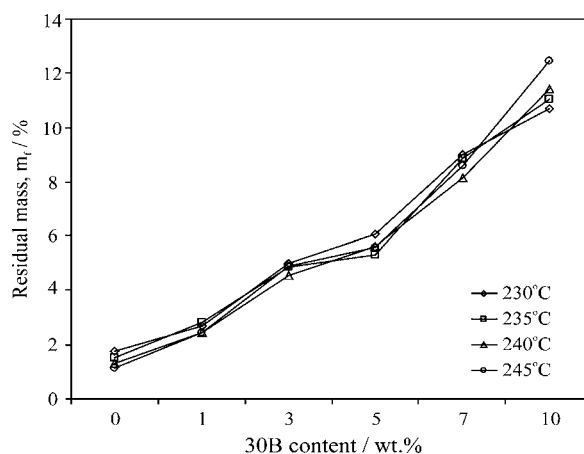
mal stability could be expected [22]. In addition, one has to take into account the fact that conformations and segmental motions of polymer chains in nanocomposites are dramatically different from those in the bulk. Chen et al. [23] have shown that nanoconfinement in both intercalated and exfoliated nanocomposites enhances intermolecular interaction so that polymer chains encounter larger energy barrier to their motion, i.e. their mobility is hindered. Hindered molecular mobility suggests a decrease in chemical reactivity or an increase in thermal stability of the nanocomposites. Chen et al. [23] also state that nanoconfinement controls the early stages of degradation and therefore contribute to the enhancement of thermal stability of polymer–clay nanocomposites at the early stages of degradation. The barrier effect occurs after the nanoconfinement has been disintegrated, i.e. at later degradation stages.

Fig. 2 shows that when the amount of 30B is over 5 wt.%, thermal stability of PHB is decreased compared to pure PHB. The possible explanation for this behaviour is the degradation of the ammonium salt used for the modification of montmorillonite [22,24,25]. Experimental results show that 30B loses 8.48, 8.93, 8.94 and 9.86 wt.% after 120 min at 230, 235, 240 and 245 °C, respectively, i.e. undergoes thermal degradation in this temperature region. It is known that the thermal degradation of ammonium salts generally proceeds by Hofmann elimination during which the ammonium cation loses an olefin and an amine and leaves an acid proton on the surface of the montmorillonite as the counterion. This acid site on the surface of the montmorillonite probably has a catalytic effect during the initial stages of PHB decomposition and is more pronounced at higher 30B loadings. Obviously, there are two opposing effects of the 30B influencing the thermal stability of PHB: ones that have positive effect and ones that have negative effect on the thermal stability of PHB, as described earlier. Up to 5 wt.% of 30B the thermal stability of PHB is improved compared to pure PHB, what indicates that activities which have negative effect on the thermal stability of PHB are either overcome or inhibited by positive ones, while at higher loadings activities which have negative effects are the dominating ones.

Residual mass of the analysed samples,  $m_f$  increases almost linearly with the amount of 30B (Fig. 3) what is expected considering the high thermal stability of 30B in this temperature region.

#### 4.2. Kinetic analysis

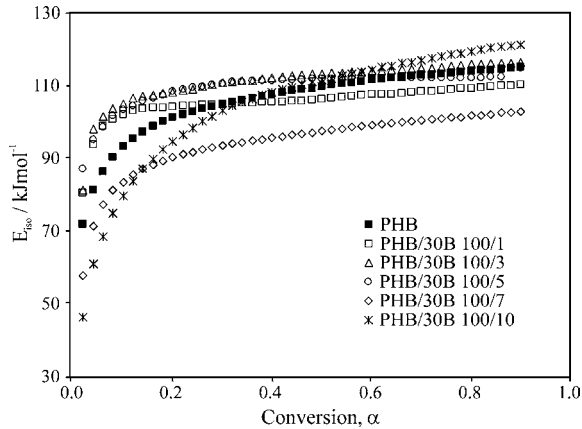
Kinetic analysis starts with the application of the *model-free* iso-conversional method (Eq. (3)). From the slopes of the straight lines  $\ln t$  vs.  $1/T$ ,  $E_{iso}$  values are obtained for each analysed sample at each selected  $\alpha$ , without assumption of kinetic model. The obtained  $E_{iso}$  values and their dependence on  $\alpha$  are shown in Fig. 4. It is concluded



**Fig. 3.** Effect of 30B content on the residual weight of PHB/30B nanocomposites.

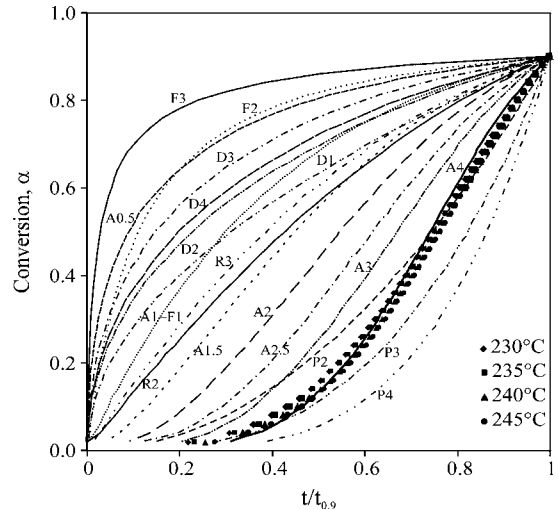
**Table 1** $E_{iso}$  values obtained by *model-free* isoconversional method in the conversion ranges where they are practically independent on  $\alpha$ .

	Sample					
	PHB	PHB/30B100/1	PHB/30B100/3	PHB/30B100/5	PHB/30B100/7	PHB/30B100/10
Conversion, $\alpha$	0.10–0.90	0.10–0.90	0.10–0.90	0.10–0.90	0.10–0.90	0.30–0.90
$E_{iso}$ (kJ mol <sup>-1</sup> )	107.9 ± 5.7	106.3 ± 2.2	112.2 ± 3.1	110.6 ± 2.4	96.1 ± 5.4	113.5 ± 5.3
$r^2$	0.99618	0.99967	0.99926	0.99436	0.99732	0.99766

**Fig. 4.** The dependence of  $E_{iso}$  on  $\alpha$  evaluated by means of *model-free* isoconversional method for pure PHB and PHB/30B nanocomposites.

from Fig. 4 that the dependence of  $E_{iso}$  on  $\alpha$  can be distinguished into two main conversion regions, the first for  $\alpha < 0.10$  in which  $E_{iso}$  increases with  $\alpha$  and the second for  $0.10 \leq \alpha \leq 0.90$  in which  $E_{iso}$  values are practically constant. This dependence of  $E_{iso}$  on  $\alpha$  indicates a complex reaction with the participation of at least two different mechanisms, which is very usual case for polymers [24,26,27]. The first part corresponds to the part where small mass loss appears ( $\alpha < 0.10$ ) while the second part, where the substantial mass loss takes place ( $0.10 \leq \alpha \leq 0.90$ ), is attributed to the main degradation mechanism. The exception is sample PHB/30B 100/10 where  $E_{iso}$  increases in the conversion range  $\alpha < 0.30$  and is practically constant in the conversion range  $0.30 \leq \alpha \leq 0.90$ .

Firstly, kinetic analysis of the main degradation mechanism is performed. Since in the conversion ranges where the main degradation mechanism occurs  $E_{iso}$  values are practically constant, the isothermal degradation of pure PHB and PHB/30B nanocomposites in these conversion ranges can be kinetically described with the unique kinetic triplet. The average  $E_{iso}$  values obtained by *model-free* isoconversional method for all investigated samples in these conversion ranges are shown in Table 1.

**Fig. 5.** Experimental RTPs for PHB/30B 100/1 nanocomposite at 230, 235, 240 and 245 °C and RTPs of the theoretical kinetic models defined in Table 2.

In order to determine the kinetic model of the main degradation mechanism, experimental and theoretical RTPs have been constructed. Fig. 5 shows experimental RTPs for PHB/30B 100/1 nanocomposite obtained at 230, 235, 240 and 245 °C in the whole conversion range. The experimental RTPs obtained at these temperatures are superimposable what indicates that the kinetic model at the specific conversion degree does not change with temperature of the isothermal degradation. The small differences are probably due to experimental uncertainties. This also means that the isothermal degradation of PHB/30B 100/1 nanocomposite in the conversion range  $0.10 \leq \alpha \leq 0.90$  can be kinetically described with the unique kinetic triplet, as concluded earlier from  $E_{iso}$  vs.  $\alpha$  dependence obtained by *model-free* isoconversional method. The experimental RTPs were compared with the RTPs of the theoretical kinetic models from Table 2, as shown in Fig. 5. The results from Fig. 5 show that Avrami-Erofeev kinetic model A4 (A4;  $g(\alpha) = [-\ln(1-\alpha)]^{1/4}$  or  $f(\alpha) = 4(1-\alpha)[- \ln(1-\alpha)]^{(1-1/4)}$ ) matches the best experimental

**Table 2**Algebraic expressions for  $f(\alpha)$  and  $g(\alpha)$  for the most frequently used mechanisms [28].

Mechanism	Symbol	$f(\alpha)$	$g(\alpha)$
Reaction order model	$F_n^a$	$(1-\alpha)^n$	$-\ln(1-\alpha)$ , for $n=1$ $(1-(1-\alpha)^{-(n+1)})/(-n+1)$ , for $n \neq 1$
Random nucleation and growth of nuclei (Avrami-Erofeev eq.)	$A_m^b$ ( $0.5 \leq m \leq 4$ )	$m(1-\alpha)[- \ln(1-\alpha)]^{(1-1/m)}$	$[- \ln(1-\alpha)]^{1/m}$
1D diffusion (parabolic law)	D1	$1/2\alpha$	$\alpha^2$
2D diffusion (bidimensional particle shape)	D2	$1/[- \ln(1-\alpha)]$	$(1-\alpha)\ln(1-\alpha) + \alpha$
3D diffusion (tridimensional particle shape) (Jander eq.)	D3	$(3(1-\alpha)^{2/3})/(2[1-(1-\alpha)^{1/3}])$	$[1-(1-\alpha)^{1/3}]^2$
3D diffusion (tridimensional particle shape) (Ginstling-Brounshtein eq.)	D4	$3/(2[(1-\alpha)^{-1/3} - 1])$	$(1-2\alpha/3) - (1-\alpha)^{2/3}$
Power law	$P_z^c$	$z\alpha^{1-1/z}$	$\alpha^{1/z}$

<sup>a</sup>  $n = 1/2$  corresponds to phase boundary controlled reaction (contracting area, R2) and  $n = 2/3$  corresponds to phase boundary controlled reaction (contracting volume, R3); also tested  $n = 2$  (F2) and  $n = 3$  (F3) kinetic models.

<sup>b</sup>  $m = 1, 2, 3$  or  $4$  when the growth rate of nuclei is proportional to the interphase area and can be 0.5; 1.5 or 2.5 in some cases of diffusion controlled growth rate of nuclei (A0.5, A1, A1.5, A2, A2.5, A3 and A4).

<sup>c</sup>  $z = 2, 3$  or  $4$  (P2, P3 or P4).

**Table 3**  
Empirical kinetic triplets obtained by RTP method for the main degradation mechanism.

Sample	Conversion, $\alpha$	$g(\alpha)$	$E$ (kJ mol <sup>-1</sup> )	$\ln A$ (min <sup>-1</sup> )	$r^2$
PHB	0.10–0.90	$[-\ln(1-\alpha)]^{1/3.33}$	111.1	23.1	0.99482
PHB/30B 100/1	0.10–0.90	$[-\ln(1-\alpha)]^{1/4.01}$	107.4	22.0	0.99966
PHB/30B 100/3	0.10–0.90	$[-\ln(1-\alpha)]^{1/3.81}$	113.9	23.7	0.99915
PHB/30B 100/5	0.10–0.90	$[-\ln(1-\alpha)]^{1/3.44}$	111.8	23.2	0.99556
PHB/30B 100/7	0.10–0.90	$[-\ln(1-\alpha)]^{1/3.03}$	98.9	20.4	0.99762
PHB/30B 100/10	0.30–0.90	$[-\ln(1-\alpha)]^{1/2.51}$	114.4	24.2	0.99773

RTPs of PHB/30B 100/1 nanocomposite among all considered theoretical kinetic models in the conversion range  $0.10 \leq \alpha \leq 0.90$ . For other investigated samples, Avrami–Erofeev kinetic models A2.5, A3 and A4 were found to match the best experimental results. Experimental RTPs of pure PHB and PHB/30B 100/5 nanocomposites were between A3 and A4 kinetic model. Kinetic models A4, A3 and A2.5 match the best experimental RTPs of PHB/30B 100/3, PHB/30B 100/7 and PHB/30B 100/10, respectively. Usually, the theoretical kinetic models cannot fit exactly the experimental results and, in our opinion, it is necessary to calculate the empirical kinetic models that emerge from the experimental results. It means that parameter “ $m$ ” of the Avrami–Erofeev kinetic model should be calculated from the experimental results. Therefore, in our case Eq. (4) turns into:

$$[-\ln(1-\alpha)]^{1/m} = kt \quad (6)$$

and after taking the natural logarithm of Eq. (6) and rearranging one obtains:

$$\ln t = \frac{1}{m} \ln[-\ln(1-\alpha)] - \ln k \quad (7)$$

Then from the slope of the plots  $\ln t$  vs.  $\ln[-\ln(1-\alpha)]$  (Eq. (7)) parameter “ $m$ ” can be obtained for each temperature of isothermal degradation. The “ $m$ ” values for PHB/30B 100/1 at 230, 235, 240 and 245 °C were 3.89, 3.97, 4.04 and 4.16, respectively, what gave the average value of 4.01, i.e.  $g(\alpha) = [-\ln(1-\alpha)]^{1/4.01}$  which is very similar to the value determined by RTP method. In the same way, parameter “ $m$ ” for all other investigated samples was determined and the obtained empirical kinetic models  $g(\alpha)$  of the main degradation mechanism are shown in Table 3. In each analysed case, straight lines with the very high correlation coefficient were obtained. The high linearity may support the suitability of the empirical kinetic model for the main degradation mechanism of the isothermal degradation of analysed samples.

From the intercept of the plots  $\ln t$  vs.  $\ln[-\ln(1-\alpha)]$  rate constant “ $-\ln k$ ” for PHB/30B 100/1 at 230, 235, 240 and 245 °C are obtained. Then, from the Arrhenius plots  $-\ln k$  vs.  $1/T$  (Fig. 6),  $E$  and

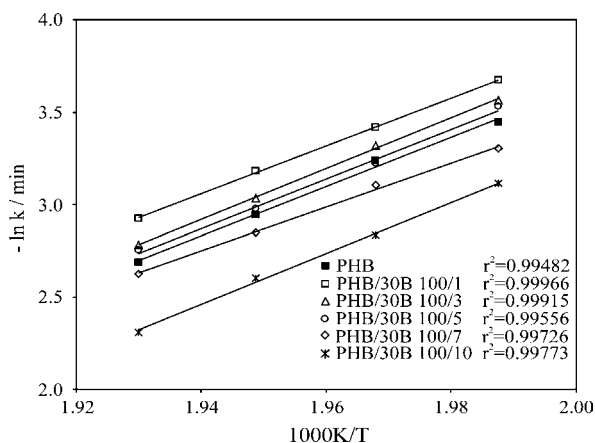


**Fig. 6.**  $-\ln k$  vs.  $1/T$  plots for pure PHB and PHB/30B nanocomposites in the conversion range  $0.10 \leq \alpha \leq 0.90$  ( $0.30 \leq \alpha \leq 0.90$  for PHB/30B 100/10).

$\ln A$  values that correspond to the empirical kinetic model were calculated from the slope and intercept, respectively, and their values are shown in Table 3. Straight lines with the very high correlation coefficient ( $r^2$ ) were obtained.

In order to check the correctness of the empirical kinetic triplets, the  $E$  values that correspond to empirical kinetic models were compared with the  $E_{iso}$  values obtained without assumption of the kinetic model [13,29]. Since the  $E$  values that correspond to empirical kinetic models (Table 3) are almost identical to  $E_{iso}$  values (Table 1), we consider that these empirical kinetic triplets can describe the main degradation mechanism very well. In this way, empirical kinetic triplets of the main degradation mechanism were calculated without any assumptions concerning kinetic model what is, as mentioned earlier, considered as the only trustworthy way of obtaining kinetic parameters.

Furthermore, Fig. 6 shows the dependence of the rate constant ( $-\ln k$ ) on 30B content and temperature of isothermal degradation. The results show that addition of 30B reduces the rate constant values compared to pure PHB when added in amounts up to 5 wt.%, i.e. reduces the rate of the isothermal degradation of PHB. The most pronounced effect has the addition of 1 wt.% of 30B what is in accordance with the earlier conclusions about influence of the 30B on the thermal stability of PHB.

Finally, the goodness of fit for each theoretical and empirical kinetic model in the conversion range  $0.10 \leq \alpha \leq 0.90$  ( $0.30 \leq \alpha \leq 0.90$  for PHB/30B 100/10) was estimated by using the residual sum of squares (Eq. (8)):

$$S_j^2 = \frac{1}{n-1} \sum_{i=1}^n \left( \frac{t_i}{t_{0.9}} - \frac{g_j(\alpha_i)}{g_j(0.9)} \right)^2 \quad (8)$$

where  $n$  is the number of data points (in our case  $n=41$ ),  $t_i$  the time required to obtain conversion  $\alpha_i$ , and  $t_{0.9}$  the time required to obtain conversion  $\alpha=0.9$ . Since the minimum value of  $S^2$  does not necessarily indicate “the most probable” kinetic model, we have performed the so-called  $F$ -test (Eq. (9)):

$$F_j = \frac{S_j^2}{S_{\min}^2} > F_{1-p, n-1, n-1} \quad (9)$$

where  $S_{\min}^2$  is the minimum value of all  $S_j^2$  and  $F_{1-p, n-1, n-1}$  is a percentile of the  $F$ -distribution for  $(1-p)100\%$  confidence probability. According to  $F$ -test, only those reaction models which obey Eq. (9) should be discriminated as giving  $S_j^2$  that are significantly larger than  $S_{\min}^2$  and therefore not belonging to the set of “the best fit” models. The reaction models which obeyed Eq. (9) fit experimental data as accurately as the model that gives  $S_{\min}^2$  [12].  $F_j$  values in Table 4 show that from the point of view of  $F$ -test the empirical and earlier mentioned theoretical Avrami–Erofeev kinetic models are “the most probable” ones (A4 for PHB, PHB/30B 100/1, PHB/30B 100/3 and PHB/30B 100/5; A3 for PHB/30B 100/7 and A2.5 for PHB/30B 100/10), although power law kinetic model P2 (P2;  $g(\alpha) = \alpha^{1/2}$ ) cannot be ruled out in case of pure PHB.

The corresponding  $E$  and  $\ln A$  values for these “the most probable” theoretical kinetic models calculated by using Eq. (4) are shown in Table 5. Since these  $E$  values significantly differ from  $E_{iso}$  values, it

**Table 4**  
Results of *F*-test for theoretical end empirical kinetic models.

<i>g</i> ( $\alpha$ )	<i>F<sub>j</sub></i> <sup>a</sup> , Sample					
	PHB	PHB/30B 100/1	PHB/30B 100/3	PHB/30B 100/5	PHB/30B 100/7	PHB/30B 100/10
EKM <sup>b</sup>	1.00	1.00	1.00	1.14	1.00	1.00
A0.5	373.90	724.69	622.53	575.22	472.33	542.54
A1 = F1	177.65	368.53	311.43	276.41	213.27	193.10
A1.5	81.21	185.22	153.04	128.40	90.19	61.92
A2	34.74	91.39	73.09	56.31	33.79	14.63
A2.5	12.81	42.74	32.48	21.68	9.50	1.13
A3	3.36	17.78	12.34	6.19	1.20	1.90
A4	1.06	1.04	1.01	1.00	4.83	18.43
R2	99.27	221.38	183.97	156.49	112.78	74.11
R3	122.71	266.01	222.50	192.43	142.48	107.05
F2	365.52	708.24	608.36	562.26	461.61	539.69
F3	501.82	948.89	819.94	768.96	645.08	823.60
D1	177.24	369.77	312.26	276.24	212.61	168.38
D2	231.41	469.21	398.84	358.79	283.18	262.32
D3	304.49	601.07	514.11	469.89	379.70	401.60
D4	256.23	514.24	438.15	396.55	315.83	308.40
P2	1.07	7.28	4.52	1.96	2.18	17.01
P3	8.34	3.83	5.15	10.79	20.74	54.35
P4	21.79	17.32	19.30	29.78	44.37	85.12

<sup>a</sup>  $F_{1-p,n-1,n-1} = 1.69$ ;  $n = 41$ ;  $p = 0.05$ .<sup>b</sup> Empirical kinetic model.**Table 5**  
*E* and *lnA* values for “the most probable” theoretical kinetic models.

Sample	Kinetic model	<i>E</i> (kJ mol <sup>-1</sup> )	<i>lnA</i> (min <sup>-1</sup> )	<i>r</i> <sup>2</sup>
PHB	A4	129.8	27.3	0.99019
	P2	129.7	27.4	0.99013
PHB/30B 100/1	A4	118.8	24.2	0.99962
PHB/30B 100/3	A4	125.8	26.4	0.99808
PHB/30B 100/5	A4	118.5	24.7	0.99696
PHB/30B 100/7	A3	114.0	23.9	0.99477
PHB/30B 100/10	A2.5	138.1	29.8	0.99837

is our opinion that empirical kinetic models are the best description for the main degradation mechanism of isothermal degradation of pure PHB and PHB/30B nanocomposites.

The same kinetic analysis has been performed for the early stage of the isothermal degradation, i.e. in the conversion range  $\alpha < 0.10$  ( $\alpha < 0.30$  for PHB/30B 100/10), in which  $E_{iso}$  values increase with  $\alpha$  (Fig. 4). The average  $E_{iso}$  values for all investigated samples in these conversion ranges are shown in Table 6.

In order to determine the kinetic model for the early stage of degradation, the experimental RTPs were compared with the RTPs of the theoretical kinetic models from Table 2, as described earlier. Fig. 5 shows that A4 and P3 (P3;  $g(\alpha) = \alpha^{1/3}$ ) kinetic models match the best experimental RTPs of PHB/30B 100/1 nanocomposites among all considered theoretical kinetic models. For other samples, the same theoretical Avrami–Erofeev kinetic models as for the main degradation mechanism and power law kinetic models (P2;  $g(\alpha) = \alpha^{1/2}$  and P3) were found to match the best experimental results. The empirical kinetic models, i.e. parameters “*m*” and “*z*” of the Avrami–Erofeev and power law kinetic models for all analysed

**Table 7**  
Values of the empirical kinetic triplets obtained by RTP method for the early stage of the isothermal degradation of pure PHB and PHB/30B nanocomposites.

Sample	Conversion, $\alpha$	<i>g</i> ( $\alpha$ )	<i>E</i> (kJ mol <sup>-1</sup> )	<i>lnA</i> (min <sup>-1</sup> )
PHB	<0.10	$[-\ln(1-\alpha)]^{1/3.31}$	122.0	25.7
		$\alpha^{1/3.23}$	123.3	25.9
PHB/30B 100/1	<0.10	$[-\ln(1-\alpha)]^{1/3.19}$	133.5	28.0
		$\alpha^{1/3.11}$	134.9	28.3
PHB/30B 100/3	<0.10	$[-\ln(1-\alpha)]^{1/2.77}$	138.7	29.3
		$\alpha^{1/2.70}$	140.3	29.6
PHB/30B 100/5	<0.10	$[-\ln(1-\alpha)]^{1/2.93}$	125.5	26.3
		$\alpha^{1/2.86}$	126.5	26.5
PHB/30B 100/7	<0.10	$[-\ln(1-\alpha)]^{1/2.76}$	119.3	25.1
		$\alpha^{1/2.69}$	121.0	25.4
PHB/30B 100/10	<0.30	$[-\ln(1-\alpha)]^{1/2.92}$	123.7	26.5
		$\alpha^{1/2.76}$	128.0	27.5

samples were calculated, respectively, together with corresponding *E* and *lnA* values (Table 7). The *E* values that correspond to empirical kinetic models are not in a good agreement with  $E_{iso}$  values for these conversion ranges. Therefore, we can conclude that the calculated empirical triplets can not kinetically describe the early stage of the isothermal degradation of PHB/30B nanocomposites. This was expected considering increasing dependence of  $E_{iso}$  on  $\alpha$ , i.e. complexity in the reaction kinetics in this conversion range. It is also known that at very low and very high conversions truly isothermal conditions can not be accomplished and therefore useful kinetic data are difficult to obtain [30]. These are probably the reasons for disagreement between isoconversional and empirical values, i.e. for

**Table 6**  
 $E_{iso}$  values obtained by model-free isoconversional method for conversion ranges in which they increase with  $\alpha$ .

	Sample					
	PHB	PHB/30B100/1	PHB/30B100/3	PHB/30B100/5	PHB/30B100/7	PHB/30B100/10
Conversion, $\alpha$	<0.10	<0.10	<0.10	<0.10	<0.10	<0.30
$E_{iso}$ (kJ mol <sup>-1</sup> )	84.3 ± 8.4	94.9 ± 8.8	97.6 ± 9.6	96.9 ± 6.4	73.8 ± 10.2	84.9 ± 16.4
<i>r</i> <sup>2</sup>	0.99886	0.99986	0.99946	0.95387	0.99293	0.99562

inability to kinetically describe isothermal degradation of PHB/30B nanocomposites in the early stage of the isothermal degradation with the unique kinetic triplet.

## 5. Conclusions

PHB/30B nanocomposites were isothermally degraded for 120 min at 230, 235, 240 and 245 °C in the nitrogen atmosphere. Addition of 30B in amounts 1–5 wt.% reduces the rate of isothermal degradation of PHB, i.e. increases its thermal stability. The most pronounced effect has the addition of 1 wt.% of 30B. From the  $E$  vs.  $\alpha$  dependence it can be concluded that the isothermal degradation of PHB/30B nanocomposites proceeds by two mechanisms: the first one corresponds to small mass loss and the second one to the main degradation mechanism where the main mass loss takes place. The first one can not be described with the unique kinetic triplet, while empirical kinetic triplets were calculated for the main degradation mechanism and they are of Avrami–Erofeev type. The  $E$  values from the empirical kinetic models agreed excellently with the  $E_{iso}$  values from the *model-free* isoconversional method what supports the calculated empirical kinetic triplets. The empirical kinetic models fit the best experimental results compared to all considered theoretical kinetic models.

It can be concluded that 30B did not affect the degradation mechanism but only the thermal stability and decomposition rate of PHB.

## Acknowledgements

The represented results emerged from the scientific project (Polymer blends with biodegradable components) financially supported by the Ministry of Science, Education and Sports of the Republic of Croatia.

## References

- [1] D.Z. Bucci, L.B.B. Tavares, I. Sell, *Polym. Test* 24 (2005) 564–571.
- [2] C. Chen, B. Fei, S. Peng, Y. Zhuang, L. Dong, Z. Feng, *Eur. Polym. J.* 38 (2002) 1663–1670.
- [3] S.N. Lee, M.Y. Lee, W.P. Park, *J. Appl. Polym. Sci.* 83 (2002) 2945–2952.
- [4] M. Erceg, T. Kovačić, I. Klarić, *Macromol. Symp.* 267 (2008) 57–62.
- [5] J. Collister, in: R. Krishnamoorti, R.A. Vaia (Eds.), *Polymer Nanocomposites: Synthesis, Characterization and Modeling*, American Chemical Society, Washington, 2001, pp. 7–14.
- [6] K.E. Strawhecker, E. Manias, *Chem. Mater.* 12 (2000) 2943–2949.
- [7] M.-A. Paul, M. Alexandre, P. Degée, C. Henrist, A. Rulmont, P. Dubois, *Polymer* 44 (2003) 443–450.
- [8] C.F. Ou, M.T. Ho, J.R. Lin, *J. Appl. Polym. Sci.* 91 (2004) 140–145.
- [9] K.M. Lee, C.D. Han, *Polymer* 44 (2003) 4573–4588.
- [10] S.V. Vyazovkin, A.I. Lesnikovich, *Thermochim. Acta* 165 (1990) 273–280.
- [11] S. Vyazovkin, C.A. Wight, *Annu. Rev. Phys. Chem.* 48 (1997) 125–149.
- [12] S. Vyazovkin, C.A. Wight, *Thermochim. Acta* 340 (341) (1999) 53–68.
- [13] S. Kim, Y. Eom, *Korean J. Chem. Eng.* 23 (2006) 409–414.
- [14] S. Akita, Y. Einaga, Y. Miyaki, H. Fujita, *Macromolecules* 9 (1976) 774–780.
- [15] <http://www.scprod.com/product.bulletins/PB%20Cloisite%2030B.pdf> (accessed on 11.09.2008).
- [16] M.J. Starink, *Thermochim. Acta* 404 (2003) 163–176.
- [17] A. Bandopadhyay, A. Ganguly, K.K. Prasad, S.B. Sarkar, H.S. Ray, *ISIJ Int.* 29 (1989) 753–760.
- [18] J.D. Sewry, M.E. Brown, *Thermochim. Acta* 390 (2002) 217–225.
- [19] N. Grassie, E.J. Murray, P.A. Holms, *Polym. Degrad. Stab.* 6 (1984) 95–103.
- [20] Y. Aoyagi, K. Yamashita, Y. Doi, *Polym. Degrad. Stab.* 76 (2002) 53–59.
- [21] M. Zanetti, G. Camino, R. Thomann, R. Müllhaupt, *Polymer* 42 (2001) 4501–4507.
- [22] A. Leszczyńska, J. Njuguna, K. Pielichowski, J.R. Banerjee, *Thermochim. Acta* 454 (2007) 1–22.
- [23] K. Chen, C.A. Wilkie, S. Vyazovkin, *J. Phys. Chem. B* 111 (2007) 12685–12692.
- [24] K. Chrissafis, G. Antoniadis, K.M. Paraskevopoulos, A. Vassiliou, D.N. Bikiaris, *Comp. Sci. Technol.* 67 (2007) 2165–2174.
- [25] A. Leszczyńska, J. Njuguna, K. Pielichowski, J.R. Banerjee, *Thermochim. Acta* 453 (2007) 75–96.
- [26] D.N. Bikiaris, K. Chrissafis, K.M. Paraskevopoulos, K.S. Triantafyllidis, E.V. Antonakou, *Polym. Degrad. Stab.* 92 (2007) 525–536.
- [27] T. Zorba, K. Chrissafis, K.M. Paraskevopoulos, D.N. Bikiaris, *Polym. Degrad. Stab.* 92 (2007) 222–230.
- [28] P. Budrugaec, E. Segal, *Int. J. Chem. Kinet.* 33 (2001) 564–573.
- [29] S. Kim, Y.C. Kim, *J. Anal. Appl. Pyrol.* 73 (2005) 117–121.
- [30] M. Maciejewski, *Thermochim. Acta* 355 (2000) 145–154.